Inorganic Chemistry

Article

pubs.acs.org/IC

Slow Magnetic Relaxation in Trigonal-Planar Mononuclear Fe(II) and Co(II) Bis(trimethylsilyl)amido Complexes—A Comparative Study

Andreas Eichhöfer,*[,†] Yanhua Lan,[‡] Valeriu Mereacre,[‡] Tilmann Bodenstein,[†] and Florian Weigend[†]

[†]Institut für Nanotechnologie, Karlsruher Institut für Technologie (KIT), Campus Nord, Hermann-von-Helmholtz-Platz 1, 76344, Eggenstein-Leopoldshafen, Germany

[‡]Institut für Anorganische Chemie, Karlsruher Institut für Technologie (KIT), Campus Süd, Engesserstr. 15, 76131, Karlsruhe, Germany

Supporting Information

ABSTRACT: Alternating current magnetic investigations on the trigonal-planar high-spin Co^{2+} complexes $[Li(15\text{-crown-5})][Co\{N(SiMe_3)_2\}_3]$, $[Co\{N(SiMe_3)_2\}_2(THF)]$ (THF = tetrahydrofuran), and $[Co\{N(SiMe_3)_2\}_2(PCy_3)]$ (Cy = $-C_6H_{13}$ = cyclohexyl) reveal that all three complexes display slow magnetic relaxation at temperatures below 8 K under applied dc (direct current) fields. The parameters characteristic for their respective relaxation processes such as effective energy barriers U_{eff} (16.1(2), 17.1(3), and 19.1(7) cm^{-1}) and relaxation times τ_0 ($3.5(3) \times 10^{-7}$, $9.3(8) \times 10^{-8}$, and $3.0(8) \times 10^{-7}$ s) are almost the same, despite distinct differences in the ligand properties. In contrast, the isostructural high-spin Fe^{2+} complexes $[Li(15\text{-crown-5})][Fe\{N(SiMe_3)_2\}_3]$ and $[Fe\{N(SiMe_3)_2\}_2(THF)]$ do not show slow relaxation of the magnetization under similar conditions, whereas the phosphine complex $[Fe\{N(SiMe_3)_2\}_2(PCy_3)]$ does, as recently reported by Lin et al. (Lin, P.-H.; Smythe, N. C.; Gorelsky, S. I.; Maguire, S.; Henson, N. J.; Korobkov, I.; Scott, B. L.; Gordon, J. C.; Baker, R. T.; Murugesu, M. *J. Am. Chem. Soc.* **2011**, *135*, 15806.) Distinctly differing axial anisotropy *D* parameters were obtained from fits of the dc magnetic data for both sets of complexes. According to density functional theory (DFT) calculations, all complexes possess spatially nondegenerate ground states. Thus distinct spin−orbit coupling effects, as a main source of magnetic anisotropy, can only be generated by mixing with excited states. This is in line with significant contributions of excited determinants for some of the compounds in complete active space self-consistent field (CASSCF) calculations done for model complexes. Furthermore, the calculated energetic sequence of d orbitals for the cobalt compounds as well as for $[Fe\{N(SiMe_3)_2\}_2(PCy_3)]$ differs significantly from the prediction by crystal field theory. Experimental and calculated (time-dependent DFT) optical spectra display characteristic d−d transitions in the visible to near-infrared region. Energies for lowest transitions range from 0.19 to 0.35 eV; whereas, for $[Li(15\text{-crown-5})][Fe\{N(SiMe_3)_2\}_3]$ a higher value is found (0.66 eV). Zero-field ^{57}Fe Mößbauer spectra of the three high-spin iron complexes exhibit a doublet at 3 K with small and similar values of the isomer shifts (δ), ranging between 0.57 and 0.59 mm/s, as well as an unusual small quadrupole splitting (ΔE_Q = 0.60 mm/s) in $[Li(15\text{-crown-5})][Fe\{N(SiMe_3)_2\}_3]$.

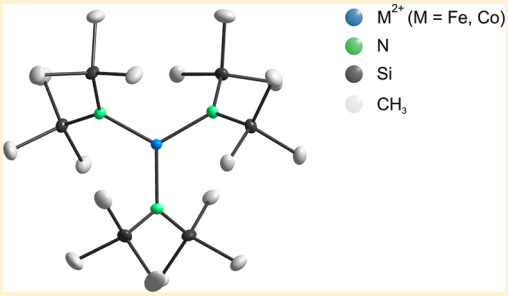

INTRODUCTION

Coordinatively unsaturated compounds of iron are of increasing interest because of their magnetic properties.[1] Three-coordinated complexes with $[LFe^{II}X]$ chromophores (L = β-diketiminate; X = -Cl, $-CH_3$, -NHTol, -NH*t*-Bu)[2] as well as two-coordinated complexes like $Fe[C(SiMe_3)_3]_2$,[3] $Fe[N(t\text{-}Bu)_2]_2$,[4] $[Fe\{N(H)Ar\}_2]$ (Ar = C_6H_3-2,6-$(C_6H_2$-2,4,6-*i*-$Pr_3)_2$ or C_6H_3-2,6-$(C_6H_2$-2,4,6-$Me_3)_2$),[5] and $[Fe(C(SiMe_3)_3)_2]^-$ display remarkably large orbital contributions to their ground-state magnetic behavior. Furthermore, zero-field Mößbauer spectra of $Fe[C(SiMe_3)_3]_2$ and $Fe[N(t\text{-}Bu)_2]_2$ at 4.2 K exhibit internal fields (H_{int}) of 152 and 105 T respectively, which are far larger than those for any other iron complex. Consequently, all of these compounds show unusual slow relaxation of the magnetization at low temperatures, with numbers for the energy barriers of the spin reversal up to 186 cm^{-1} in $[Fe\{N(SiMe_3)(Dipp)\}_2]$ (Dipp = C_6H_3-2,6-*i*-Pr).[6,7] Such single-ion molecule magnet behavior, which was first observed in lanthanide-containing complexes,[8,9] was also reported for several first-row transition metal complexes of iron[10−12] and cobalt[13−15] for different coordination geometries including the trigonal-planar complex $[Fe\{N(SiMe_3)_2\}_2(PCy_3)]$ (Cy = cyclohexyl).[16] Slow magnetic relaxation at a zero dc (direct current) field was for the first time observed in the PPh_4^+ salt of the tetrahedral cobalt thiolate complex $[Co(SPh)_4]^{2-}$.[14]

Mononuclear three-coordinate complexes of Fe^{2+} and Co^{2+} are for example accessible as Lewis base adducts of well-known homoleptic bis(trimethylsilyl)amide complexes $[M\{N(SiMe_3)_2\}_2]$ (M = Co[17,18] and Fe[19,20]) like $[Fe\{N(SiMe_3)_2\}_2(PCy_3)]$,[16] $[Fe\{N(SiMe_3)_2\}_2(THF)]$ (THF = tetrahydrofuran),[19,20] $[Co\{N(SiMe_3)_2\}_2(PPh_3)]$[21], and $[M\{N(SiMe_3)_2\}_2$

Received: July 3, 2013
Published: January 27, 2014

   dx.doi.org/10.1021/ic401677j | *Inorg. Chem.* 2014, 53, 1962−1974

(py)] (M = Fe, Co; py = pyridine),[22] or as anions in [Na(12-crown-4)$_2$] [M{N(SiMe$_3$)$_2$}$_3$] (M = Fe, Co).[23] First-row transition-metal silylamides have been shown to be generally useful precursors for a wide variety of derivatives of these metals.[24−27] Investigation of transition-metal amides in our laboratory originally stems from the interest to utilize them as precursor complexes for the synthesis of mixed metal chalcogenide cluster complexes[28] as well as the synthesis of polymeric metal chalcogenolato complexes.[29]

Herein we report on the synthesis and structural as well as physical characterization of three trigonal-planar Co^{2+} bis-(trimethylsilyl)amido complexes, in comparison to their Fe^{2+} analogues, with a focus on their magnetic properties.[30]

RESULTS AND DISCUSSION

Synthesis and Structure. The complexes [Li(15-crown-5)] [M{N (SiMe$_3$)$_2$}$_3$] (M = Fe(**1**), Co(**2**)) were synthesized in good yields by the reaction of [M{N(SiMe$_3$)$_2$}$_2$]$_2$ (M = Fe,[19] Co[17]) with lithium bis(trimethylsily)amide in toluene in the presence of 15-crown-5 as reported for the amido complexes [Li(12-crown-4)$_2$] [M{N(SiMe$_3$)$_2$}$_3$] (M = Mn, Fe, Co)[23] (see Scheme 1).

Scheme 1

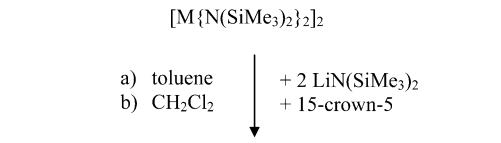

Intensely green [Co{N(SiMe$_3$)$_2$}$_2$ (THF)] (**4**)[30] and green [Co{N(SiMe$_3$)$_2$}$_2$ (PCy$_3$)] (**6**) were synthesized by the recrystallization of [Co{N(SiMe$_3$)$_2$}$_2$]$_2$ in THF and from toluene in the presence of 2 equiv of tricyclohexylphosphine, respectively (see Scheme 2).

Scheme 2

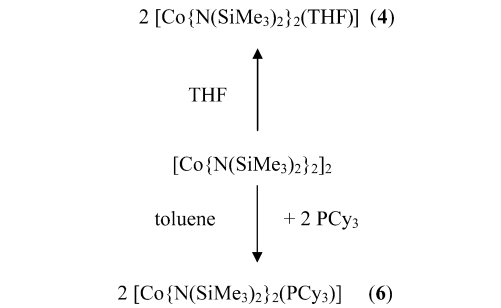

To do a comparative study, we also reproduced the reported isostructural iron compounds [Fe{N(SiMe$_3$)$_2$}$_2$(L)] (L = THF (**3**)[19,20] and L = PCy$_3$ (**5**)[16]). The detailed synthetic procedures can be found in the Experimental Section.

The ionic complexes **1** and **2** crystallize both in the monoclinic space group $P2_1/n$ (Table 1), with one CH_2Cl_2 molecule in the asymmetric unit. The cations are built by dimerization of two [Li(15-crown-5)]$^+$ units, a structural motif that has not been observed before (Supporting Information, Figure S1). In the monomeric anions [M{N(SiMe$_3$)$_2$}$_3$]$^-$ (M = Fe (**1a**), Co(**2a**)) the metal ions are planary coordinated by the three nitrogen atoms of the bis(trimethylsilyl)amido groups (Figure 1). The symmetry of the complexes is slightly distorted from an idealized D_3 point group symmetry (for bond distances

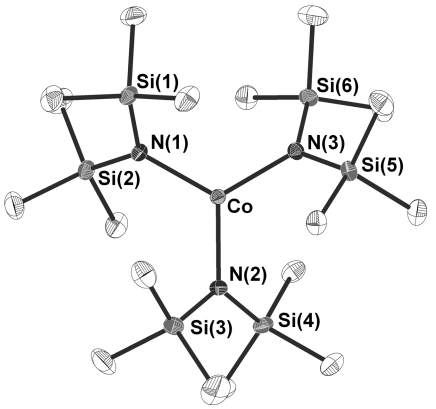

Figure 1. Molecular structure of the anion [Co(N(SiMe$_3$)$_2$)$_3$]$^-$ (**2a**) in the crystal of **2** (30% ellipsoids, H atoms omitted for clarity). Selected bond lengths [pm] and angles [deg]: Co(1)−N(1) 196.9(2), Co(1)−N(2) 197.4(2), Co(1)−N(3) 197.5(2), N(1)−Co(1)−N(2) 119.63(9), N(1)−Co(1)−N(3) 120.78(9), N(2)−Co(1)−N(3) 119.59(9). Selected bond lengths [pm] and angles [deg] for isostructural [Fe(N(SiMe$_3$)$_2$)$_3$]$^-$ (**1a**): Fe(1)−N(1) 198.4(2), Fe(1)−N(2) 198.9(2), Fe(1)−N(3) 198.9(2); N(1)−Fe(1)−N(2) 119.75(9), N(1)−Fe(1)−N(3) 120.66(9), N(2)−Fe(1)−N(3) 119.58(9).

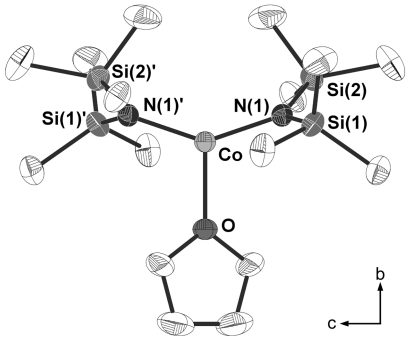

Figure 2. Molecular structure of [Co(N(SiMe$_3$)$_2$)$_2$ (THF)] (**4**) in the crystal along *a* (30% ellipsoids, H atoms are omitted for clarity). Symmetry transformation for generation of equivalent atoms: 1−x, y, −z+3/2. Selected bond lengths [pm] and angles [deg]: Co(1)−N(1) 189.8(2), Co(1)−N(1)′ 189.8(2), Co(1)−O(1) 203.6(3), N(1)−Co(1)−N(1)′ 141.78(12), N(1)−Co(1)−O(1) 109.11(6), N(1)′−Co(1)−O(1) 109.11(6).

and angles see figure caption). With respect to the structures of the isostructural M(III) neutral molecules [M{N(SiMe$_3$)$_2$}$_3$] (M = Fe,[31] Co[17]) one observes extended M−N bond distances in **1** and **2** (M = Fe, ∼7 pm; M = Co, ∼10 pm). This was also observed before for isostructural [Li(12-crown-4)$_2$] [M{N-(SiMe$_3$)$_2$}$_3$] and related to the larger ionic radii of the metal ions in **1** and **2** as well as a weakening of the M−N bond by the excess charge.[23]

Complex **4** crystallizes in the orthorhombic space group *Pbcn* (Table 1); the molecular structure of **4** is shown in Figure 2. A crystallographically imposed 2-fold axis is running through the Co−O bond. The cobalt atom is coordinated by two bis(trimethylsilyl)amido and one THF ligand in a distorted trigonal-planar geometry. The Co−N distances (189.8(2) pm) are shorter than the Co−O bond length (203.6(3) pm), and the N−Co−N angle (141.78(12)°) is much larger than the two

dx.doi.org/10.1021/ic401677j | Inorg. Chem. 2014, 53, 1962−1974

O−Co−N angles (109.11(6)°). Complex **4** is isostructural to the corresponding iron compound **3**, which diplays only slightly different structural parameters (Fe−N: 191.6(5), Fe−O 207.1(6) pm; N−Fe−N: 144.0(3), O−Fe−N 108.0(1)°).[19]

Complex **6** crystallizes in the monoclinic space group $P2_1/n$ (Table 1). Two bis(trimethylsilyl)amido ligands and the tricyclohexyl phosphine ligand form a distorted trigonal-planar geometry around the cobalt atom (Figure 3). The Co−N

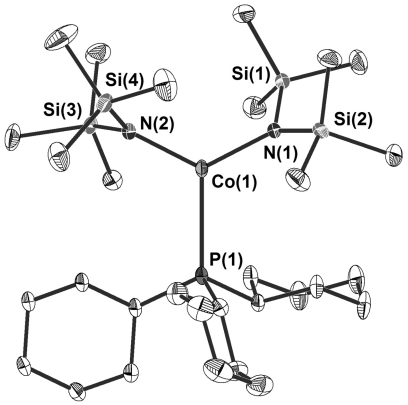

Figure 3. Molecular structure of $[Co(N(SiMe_3)_2)_2(PCy_3)]$ (**6**) in the crystal (30% ellipsoids, H atoms omitted for clarity). Selected bond lengths [pm] and angles [deg]: Co(1)−N(1) 192.9(2), Co(1)−N(2) 192.3(2), Co(1)−P(1) 251.8(1), N(1)−Co(1)−N(2) 125.44(8), N(1)−Co(1)−P(1) 117.49(9), N(2)−Co(1)−P(1) 117.03(6).

distances (192.3(2), 192.9 pm) are distinctly shorter than the Co−P bond length (251.8(1) pm), and the N−Co−N angle (125.44(8)°) is larger than the two P−Co−N angles (117.03, 117.49(6)°). The cobalt complex **6** is isostructural to the recently published iron compound **5**, which only displays slightly different structural parameters (Fe−N: 195, 195; Fe−P 252 pm; N−Fe−N: 128.5, P−Fe−N 115.2, 116.3°).[16]

In comparison, structural differences between the cobalt and the iron analogues are restricted to the slightly smaller ionic radius of Co^{2+} in comparison to Fe^{2+} (Fe^{2+}, high-spin, CN 4, 77 pm; Co^{2+}, high-spin, CN 4, 72 pm).[32] Upon going from **1** to **3** to **5** and from **2** to **4** to **6**, the molecular point group symmetry of the complexes is reduced from D_3 over C_2 to C_1. Deflexions of the metal atoms from the trigonal plane formed by the coordinating ligand atoms are small (**1**: 0.72(12), **2**: 0.66(13), **3**: 0,[20] **4**: 0, **5**: 3.0,[16] **6**: 2.6(1) pm). The shortest interatomic distances between the metal atoms in the crystal lattices were found to range from 874 to 924 pm (**1**: 894.0, **2**: 896.0, **3**: 873.7, **4**: 880.2, **5**: 923.7, **6**: 916.8 pm).

The measured powder patterns of **1**−**6** show a good agreement with the calculated ones based on the single crystal data (Figures S2−S7 in the Supporting Information), which proves the crystalline purity of the compounds.

Magnetic Behavior. For all complexes **1**−**6**, dc and ac (alternating current) magnetic properties have been studied on crystalline powders. Taking into account the extreme air and moisture sensitivity of the compounds, we prepared the dc measurements of each compound on several samples of different batches till we obtained at least two reproducible measurements. For those we proceeded to carry out the ac and temperature-dependent magnetization measurements.

Static magnetic behavior of complexes **1**−**6** were studied between 1.8 and 300 K in a field of 0.1 T and by magnetization measurements from 0 to 5 T at 2, 3, 4, 5, and 6 K. The μ_{eff} versus T and **M** versus H curves at different temperatures were simultaneously fitted using the PHI program[33] by means of an anisotropic spin Hamiltonian (SH) (with $g_x = g_y$):

Table 1. Crystallographic Data for $[Li(15\text{-crown-}5)][M\{N(SiMe_3)_2\}_3]$ (M = Fe (1), Co(2)), $[Co\{N(SiMe_3)_2\}_2(THF)]$ (4),[30] and $[Co\{N(SiMe_3)_2\}_2(PCy_3)]$ (6)

	1·CH_2Cl_2	**2**·CH_2Cl_2	**4**	**6**
sum formula	$C_{29}H_{76}Cl_2FeLiN_3O_5Si_6$	$C_{29}H_{76}Cl_2CoLiN_3O_5Si_6$	$C_{16}H_{44}CoN_2OSi_4$	$C_{30}H_{69}CoN_2Si_4P$
fw [g/mol]	849.16	852.24	451.82	660.14
crystal system	monoclinic	monoclinic	orthorhombic	monoclinic
space group	$P2_1/n$	$P2_1/n$	*Pbcn*	$P2_1/n$
cell *a* [pm]	1461.4(3)	1461.4(3)	1360.9(3)	1725.4(4)
b	2052.3(4)	2049.4(4)	1116.5(2)	1178.1(2)
c	1671.0(3)	1672.7(3)	1781.9(4)	2081.0(4)
β [°]	107.77(3)	108.03(3)		111.33(3)
V [10^6pm^3]	4772.6(18)	4763.9(16)	2707.6(9)	3940.2(14)
Z	4	4	4	4
T [K]	180(2)	180(2)	180(2)	180(2)
d_c [g cm^{-3}]	1.182	1.188	1.108	1.113
$\mu(\lambda)$ [mm^{-1}]	0.613	0.657	0.817	0.618
F[000]	1832	1836	980	1444
$2\theta_{max}$ [deg]	52	54	52	51
meas reflns	22 197	35 936	15 163	26 244
unique reflns	8890	10 070	2554	7394
R_{int}	0.0350	0.0811	0.0446	0.0992
reflns with $I > 2\sigma(I)$	6878	7071	1867	5950
refined params	421	439	146	499
$R1(I > 2\sigma(I))^a$	0.0461	0.0470	0.0376	0.0421
$wR2$(all data)^b	0.1279	0.1304	0.1086	0.1183

$^a R1 = \sum||F_o|-|F_c||/\sum|F_o|$. $^b wR2 = [\sum[w(F_o^2 - F_c^2)^2]/\sum[w(F_o^2)^2]]^{1/2}$.

dx.doi.org/10.1021/ic401677j | Inorg. Chem. 2014, 53, 1962−1974

$$\hat{H} = D(\hat{S}_z^2 - 1/3\hat{S}) + E(\hat{S}_x^2 - \hat{S}_y^2) + \mu_B(\hat{S}_x g_x B_x + \hat{S}_y g_y B_y + \hat{S}_z g_z B_z) \quad (1)$$

where D = axial ZFS parameter, E = rhombic ZFS parameter, $\hat{S}$ = spin operator, $\boldsymbol{B}$ = magnetic induction, g = Landé factor, and μ_B = Bohr magneton.

It is known that the reliability of such a model depends on the electronic structure of the system under study, particularly in the presence of (near-)degeneracies.[34] For the complexes **1**−**6**, density functional theory (DFT) calculations reveal that the ground state of each complex exhibits an orbital quantum number $L = 0$ (see section Theory). Thus nonvanishing contributions to L can only be generated by mixing with excited states.[35] To estimate the reliability of the SH parameters, we refer to the complete active space self-consistent field (CASSCF) and spin−orbit configuration interaction (SOCI) calculations (see section Theory). The amount of mixing and thus the estimated reliability of eq 1 at this level of theory is quantified in the third column of Table 4: large contributions of excited determinants indicate that strong spin−orbit effects may occur, and hence the (perturbative) SH in eq 1 might be only a crude approximation in these cases. Dynamic magnetic properties were probed in ac measurements performed in the 1.8−10 K range using a 3.0 Oe oscillating ac field at frequencies between 1 and 1500 Hz. From the frequency dependence of the out-of-phase signal under an applied dc field at different temperatures, the relaxation time τ was extracted by fits to eq 2 in the Supporting Information (Tables S1, S4, and S6). The energy barriers U_{eff} for reversal of magnetization direction were obtained according to Glauber's theory,[36] where the thermal variation of τ is described by an Arrhenius expression (eq 4 in the Supporting Information) with τ_0 being a pre-exponential. Below, we will first discuss the dc and ac magnetic properties of the cobalt complexes **2**, **4**, and **6**, followed by those of their iron analogues **1**, **3**, and **5**.

The effective magnetic moments (μ_{eff}) of **2**, **4**, and **6** continuously decrease with decreasing temperature (Figure 4a). This deviation from the ideal Curie behavior is in the absence of any close Co···Co contacts likely attributable to magnetic anisotropy, which is indicative of a significant ZFS and g-factor anisotropy resulting from the pseudotrigonal crystal field. Magnetic anisotropy is also indicated by the room temperature values of μ_{eff}, which are much larger than the theoretical spin-only value of 3.87 μ_B mol^{-1} for one Co^{2+} ion (high-spin, $S = 3/2$), which in turn results in the large g values derived from the μ_{eff} at room temperature. Comparable large values for μ_{eff} at room temperature have been reported for $[Co(N(SiMe_3)_2)_2(THF)]$ (5.88 μ_B mol^{-1})[30] and other three-coordinated Co^{2+} complexes $[Co(N(SiMe_3)_2)_2(PMe_3)]$ (4.71 μ_B mol^{-1}),[30] $[Co(N(SiMe_3)_2)_2(PPh_3)]$ (4.84 μ_B mol^{-1}),[21] $[Co(N(SiMe_3)_2)_2(py)]$ (4.69[22], 5.27[30] μ_B mol^{-1}), and $[Na(12\text{-crown-}4)]_2[Co(N(SiMe_3)_2)_3]$ (5.75 μ_B mol^{-1}).[30] The field dependence of the magnetization (**M**) of **2**, **4**, and **6** at 2 K displays similar curves (Supporting Information, Figure S8), which suggests similar ground states of the molecules as also supported by the similar values of μ_{eff} at 2 K. The lack of saturation (M_S ($S = 3/2$) = 3 N μ_B) is also indicative of magnetic anisotropy in all three complexes.

To probe this magnetic anisotropy further, we performed least-squares fits to eq 1 as described above. The fittings are in general quite good. The best sets of parameters are listed in Table 2 and shown as solid lines in Figure 4a and Figure S9 in the Supporting Information. All three cobalt complexes display anisotropic g parameters and large negative D values. The g values for **4** and **6** are anisotropic, with $g_x = g_y < g_z$, whereas similar fits of the g factor of **2** resulted in $g_x = g_y > g_z$. Quite similar anisotropic g values like those in **2** have been reported recently for $[Na(14\text{-crown-}4)]_2[Co(N(SiMe_3)_2)_3]$ ($g_x = g_y = 2.97$, $g_z = 2.75$).[30] However, this is in view of the large negative D value (and a negative spin−orbit coupling parameter λ for Co^{2+} (d^7)) not in line with the "consistency criterion" derived from perturbation theory which requires $D = 0.5\lambda(g_z - g_x)$.[37] For $S = 3/2$ ions, χT curves are known to be insensitive to the sign of D;[37,69] whereas, they are not when coupled by an E parameter and simultaneously fit with temperature-dependent magnetization data. Reasonable fits ($R = 7.72 \times 10^{-4}$) with a positive $D = 46.3$ cm^{-1} resulted in $g_x = g_y = 2.73 < g_z = 3.13$ (also not consistent with the above formula) and in significantly increased E values ($E = \pm 17.4$ cm^{-1}), which gives rise to an $E/D > 1/3$. Therefore the data of **2** were fitted with an isotropic g factor and a negative $D = -57$ cm^{-1}, which slightly deteriorates the goodness of fit but results in a "proper"[38] $E/D < 1/3$ (not the case for positive D and isotropic g). Comparable large D and E values have been found for trigonal-planar as well as for

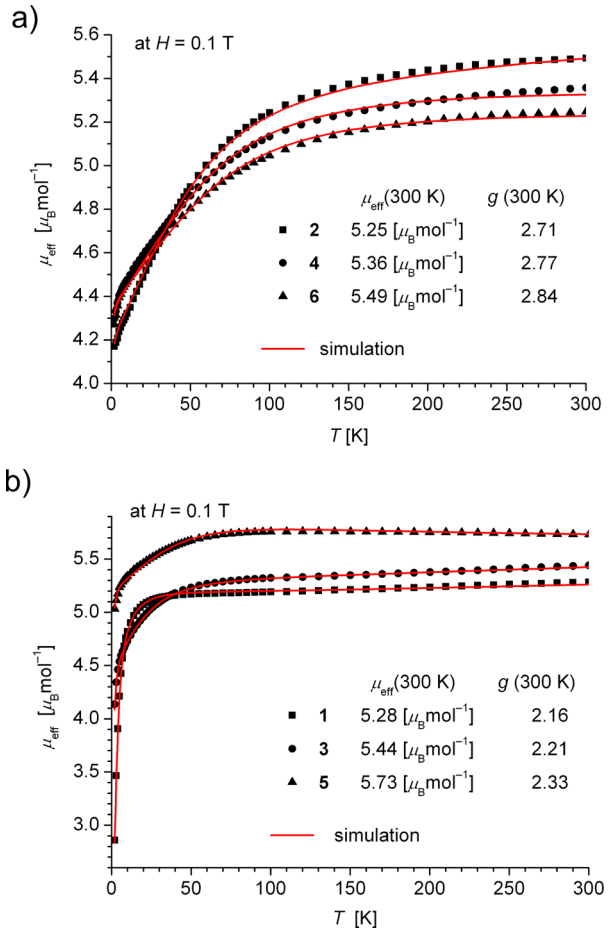

Figure 4. Temperature dependence of the magnetic moment (μ_{eff}) of (a) $[Li(15\text{-crown-}5)][Co(N(SiMe_3)_2)_3]$ (**2**), $[Co(N(SiMe_3)_2)_2(THF)]$ (**4**), $[Co(N(SiMe_3)_2)_2(PCy_3)]$ (**6**), and (b) $[Li(15\text{−crown−}5)][Fe\{N(SiMe_3)_2\}_3]$ (**1**), $[Fe\{N(SiMe_3)_2\}_2(THF)]$ (**3**), $[Fe\{N(SiMe_3)_2\}_2(PCy_3)]$ (**5**). Solid lines represent the results of the simultaneous fittings with the temperature-dependent magnetization (Table 2, Figures S8 and S22 in the Supporting Information), according to a spin Hamiltonian (eq 1) by the PHI program.[33]

dx.doi.org/10.1021/ic401677j | Inorg. Chem. 2014, 53, 1962−1974

Table 2. Results of the Fittings of the DC Magnetic Data[a] by the PHI Program[33] and of the Evaluation of the AC Magnetic Data[b] of 1−6[c]

	$g_x = g_y$	g_z	D [cm^{-1}]	E [cm^{-1}]	R [10^{-3}]	H_{dc} [Oe]	U_{eff} [cm^{-1}]	τ_0 [s]
[Li(15-crown-5)] [Co{N(SiMe$_3$)$_2$}$_3$] (**2**)[d]	2.79	2.79	−57	±12.7	3.32	800	16.1(2)	3.5(3) × 10^{-7}
[Co{N(SiMe$_3$)$_2$}$_2$ (THF)] (**4**)	2.68	2.90	−72	±13.5	0.003	600	18.1(3)	9.3(8) × 10^{-8}
[Co{N(SiMe$_3$)$_2$}$_2$ (PCy$_3$)] (**6**)	2.58	2.90	−82	±0	0.85	750	19.1(7)	3.0(8) × 10^{-7}
[Li(15-crown-5)] [Fe{N(SiMe$_3$)$_2$}$_3$] (**1**)[e]	2.18	1.91	+9.9	±0.0	0.006	0−1000		
[Fe{N(SiMe$_3$)$_2$}$_2$ (THF)] (**3**)[e]	2.07	2.28	−20	±4.0	0.25	0−1000		
[Fe{N(SiMe$_3$)$_2$}$_2$ (PCy$_3$)] (**5**)	2.14	2.61	−33	±3.4	3.15	600	16.0(3)	1.6(2) × 10^{-6}

[a]Simultaneous treatment of χT vs T and **M** vs H plots at different temperatures (Figure 4 and Figures S9 and S23 in the Supporting Information). [b]Figure 5 and S27 in the Supporting Information. [c]Parameters: g, uniaxial magnetic anisotropy D, transversal magnetic anisotropy E, goodness-of-fit factor R (least-square approach), external magnetic field H_{dc}, effective energy barrier U_{eff} and relaxation time τ_0. [d]A TIP of 0.0005 cm^3 mol^{-1} has been considered in the simulation of the μ_{eff} vs T data of **2**; Landé factor g refined isotropic (see text). [e]A TIP of 0.0005 and 0.0007 cm^3 mol^{-1} has been considered in the simulation of the μ_{eff} vs T data of **1** and **3** respectively.

pentacoordinated Co^{2+} complexes: [Co(N(SiMe$_3$)$_2$)$_2$ (THF)] (D = −73 cm^{-1}, E = ±14.6 cm^{-1}), [Co(N(SiMe$_3$)$_2$)$_2$ (PMe$_3$)] (D = −74 cm^{-1}, E = ±9.6 cm^{-1}), [Co(N(SiMe$_3$)$_2$)$_2$ (py)] (D = −82 cm^{-1}, E = ±21.0 cm^{-1}), [Na(12-crown-4)]$_2$ [Co(N-(SiMe$_3$)$_2$)$_3$] (D = −62 cm^{-1}, E = ±10.0 cm^{-1}),[30] [Co(bzimpy)-Cl$_2$] (bzipym = 2,6-bis{benzimidazol-2′-yl}-pyridine) (D = 73.4 cm^{-1}, E = ±3.28 cm^{-1})[39], and octahedral [Co(iphos)$_2$ (H$_2$O)$_2$] (iphos = imino-bis{methylphophosphonate}) (D = 52 cm^{-1}, E = ±17 cm^{-1}).[40] The large g-factor variations and D values found for the cobalt complexes are indicative of the presence of strong spin−orbit coupling contributions as recently outlined.[35,41,42] It was already mentioned above that these are not considered by the Hamiltonian (eq 1) used in the fittings. Therefore fittings according to eq 1 might incorporate spin−orbit interactions (including first-order terms) into D on the one hand and into the principal values of g_z and g_x of the g matrix on the other hand, which depends on the degree of admixture of excited determinants (see Table 4).

The dynamic magnetic behavior of **2**, **4**, and **6** in terms of the ac measurements is shown in Figure 5a and in the Supporting Information, Figures S10−S21. In the absence of an external dc field, the out-of-phase component of the ac susceptibility (χ'') of **2**, **4**, and **6** has a much lower intensity than the in-phase component (χ'), which indicates fast zero-field tunneling of the magnetization.[43,44] With the application of a static dc field the intensity of χ'' is significantly enhanced for all three cobalt complexes **2**, **4**, and **6** and reaches a similar order to that of χ'. This effect is ascribed to a removal of the state degeneracy by the dc field, which helps to suppress or slow down the relaxation process through quantum tunneling.[45,46] It is worthwhile to mention that for compound **2** there is an indication of a second relaxation process occurring at higher frequencies (Supporting Information, Figure S10). This might be attributed to a partial desolvation during the sample preparation which leads to multiple species present in the probe with slightly different relaxation barriers. The relaxation time of **2**, **4**, and **6** versus the inverse temperature, plotted in Figure 5b, shows a curvature feature down to low temperatures suggesting a crossover from thermally activated relaxation processes to those which are associated with quantum tunneling of the magnetization. The data at higher temperatures which correspond to the thermally activated process follows an Arrhenius law, leading to almost the same sets of parameters (Table 2). These values are comparable to those of recently reported examples such as the distorted square pyramidal complexes [{ArN═CMe}$_2$ (NPh)]Co(NCS)$_2$ (U_{eff} = 11.1 cm^{-1}, τ_0 = 3.6 × 10^{-6} s) and [{ArN═CPh}$_2$ (NPh)]Co-(NCS)$_2$ (U_{eff} = 16.7 cm^{-1}, τ_0 = 5.1 × 10^{-7} s),[13] the tetrahedral complex [Co(SPh)$_4$]$^{2-}$ (U_{eff} = 21 cm^{-1}, τ_0 = 1.0 × 10^{-7} s),[14] and the pseudotetrahedral complex [(3G)CoCl]$^-$ (1; 3G = 1,1,1-tris-[2N-(1,1,3,3-tetramethylguanidino)methyl]ethane) (U_{eff} = 24 cm^{-1}, τ_0 = 1.9 × 10^{-10} s).[15] The relaxation times in the order of 10^{-7} s are typical for an Orbach process. From

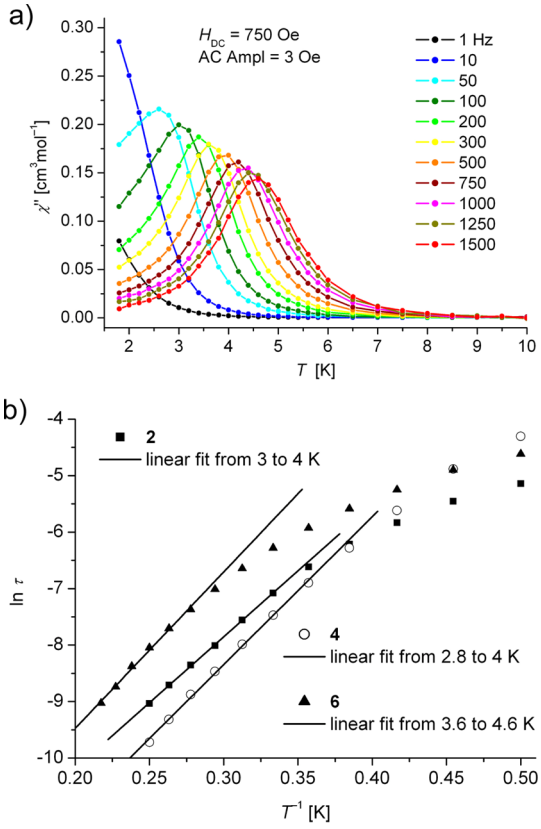

Figure 5. (a) Temperature dependence of the out-of-phase χ'' component of the ac magnetic susceptibility at 750 Oe at different frequencies for [Co{N(SiMe$_3$)$_2$}$_2$ (PCy$_3$)] (**6**) (solid lines are a guide for eyes). (b) Relaxation time (τ) versus the inverse temperature (T^{-1}) for [Li(15-crown-5)] [Co(N(SiMe$_3$)$_2$)$_3$] (**2**), [Co(N(SiMe$_3$)$_2$)$_2$ (THF)] (**4**), and [Co(N(SiMe$_3$)$_2$)$_2$ (PCy$_3$)] (**6**). Standard deviations of the relaxation times were determined from a nonlinear least-squares analysis using the program Origin R (Version 6.1, OriginLab Cooperation, 1991−2000); the error of ln τ was estimated from that of τ by eq 6 in the Supporting Information. Error bars are omitted as they are within the radius of the symbols. Linear fits represent Arrhenius laws (eq 4 in the Supporting Information) and are shown as solid lines (for corresponding parameters, see Table 3).

dx.doi.org/10.1021/ic401677j | Inorg. Chem. 2014, 53, 1962−1974

least-squares fittings of the plots of χ'' versus χ' (known as Cole−Cole plots, Supporting Information, Figures S13, S17, and S21) onto a distribution of single relaxation processes (Debye model, eq 3 in the Supporting Information) the distribution coefficients α could be derived (Tables S3, S5, and S7). For all complexes, values of $\alpha < 0.2$ were found which is indicative for small distributions of single relaxation processes.

The room temperature μ_{eff} (5.4, 5.3, and 5.7 μ_B mol^{-1}) of all three iron complexes **1**, **3**, and **5** are found to be larger than the theoretical spin-only value of 4.9 μ_B mol^{-1} for one Fe^{2+} ion (high-spin, $S = 2$) (Figure 4b). The g values derived from the μ_{eff} at room temperature for the $S = 2$ complexes amount to 2.16 (**1**), 2.20 (**3**) and 2.33 (**5**). However the enhancement is not pronounced as strong as for the cobalt complexes which might be understood by use of the equation $g_{eff} = g_e - \alpha \times \lambda/10Dq$, which quantifies the "$g$-factor variation" assuming isotropic behavior and no first-order orbital angular momentum.[53] Both ground terms of the free ions (Co^{2+}, $^4F_{9/2}$; Fe^{2+}, $^5D_4$) split in a trigonal-planar ligand field of D_{3h} point group symmetry to give an A ground term, for which $\alpha = 4.10Dq$ is expected to be almost the same for each pair of similar ligated complexes, so that only the difference between the spin−orbit coupling constants of the free ions of Co^{2+} (−177 cm^{-1}) and Fe^{2+} (−102 cm^{-1}) remains.[47] The experimental μ_{eff} of **1** and **3** are comparable to that of the reported three-coordinate complex [Fe(N(SiMe$_3$)$_2$)$_2$(py)] (5.3 μ_B mol^{-1}),[22] whereas **5** displays a higher value, although not as high as recently reported (6.4 μ_B mol^{-1}).[16] When the compounds are cooled from 300 to 100 K, the μ_{eff} of **1** and **3** slightly decrease, while that of **5** slightly increases (Figure 4b). Below 50 K, **3** and **5** display a rapid downturn of the magnetic moment with further decreasing temperature, which is, in the absence of any close M···M contacts, indicative for the presence of zero-field splitting (ZFS) of the spin states in these complexes.[16,10] In contrast, **1** does not display such an early deviation from ideal Curie behavior. In agreement with distinctly different values of μ_{eff} at 2 K (2.9, 4.1, and 5.0 μ_B mol^{-1}), the curves of the field dependence of the magnetization (**M**) of **1**, **3**, and **5** at this temperature are also different (Supporting Information, Figure S22). This behavior suggests either different ground states for these complexes or distinct different magnetic anisotropies or both. The lack of saturation (M_S ($S = 2$) = 4 N μ_B) at high field is quite pronounced for **1** which in principle indicates less influence of magnetic anisotropy. The best sets of parameters of simultaneous least-squares fittings of the μ_{eff} versus T and M versus H curves at different temperatures using eq 1 are listed in Table 2 and shown as solid lines in Figure 4 and Figure S23 in the Supporting Information. The g and D values of **1**, **3**, and **5** obtained in this way differ significantly. Fits of the anisotropic g-factor of **1** resulted in $g_x = g_y > g_z$ which is in view of the positive $D = +9.9(1)$ cm^{-1} in agreement with the consistency criterion mentioned before.[37] The value of $g_z = 1.91$ however is unusual for a high-spin Fe^{2+} compound.[37] In contrast the D value of **3** is found to be negative ($D = -20(1)$ cm^{-1}) similar to values reported for the three-coordinated complexes [(IPr)Fe{N(SiMe$_3$)$_2$}$_2$] (IPr = 1,3-bis(diisopropylphenyl)imidiazol-2ylidene) ($g = 2.27$, $D = -18.2$ cm^{-1}) and [[(IMes)Fe{N(SiMe$_3$)$_2$}$_2$] (IMes =1,3-bis(2,4,6-trimethylphenyl)-imidiazol-2ylidene) ($g = 2.24$, $D = -23.3$ cm^{-1}).[48] **5** displays distinctly larger values of $g_z = 2.61$ and $D = -33.0$ cm^{-1} together with a moderate $E = \pm 3.4$ cm^{-1}. Again strong mixing with excited determinants in the case of **3** and **5** (Table 4) suggest that the ZFS parameters of theses complexes include the influence of strong spin−orbit interaction while those of **1** (almost no mixing with excited determinants) are thought to be reliable.

In agreement with the findings from the static properties, the dynamic magnetic behavior of the iron compounds **1**, **3**, and **5** also reveals pronounced differences between the different types of molecules. Ac measurements performed under similar conditions as for the cobalt analogues display no out-of-phase signals χ'' for **1** and **3** even if an external dc field is applied up to 0.1 T. The absence of slow relaxation of magnetization for complex **1** is in line with the positive D value. However, it should be mentioned that typical single-molecule magnet behavior has also been observed under an applied field for mononuclear cobalt complexes that have a positive ZFS.[15,49] In contrast, a field-induced slow relaxation of magnetization was observed in complex **5** similar to that reported.[5] The characteristic parameters of the relaxation process are determined as $U_{eff} = 16.0(3)$ cm^{-1} and $\tau_0 = 1.6(2) \times 10^{-6}$ s from our experimental data (Supporting Information, Figures S24−S28), which differ from those in reference 16 ($U_{eff} = 29.2$ cm^{-1}, $\tau_0 = 6.0 \times 10^{-7}$ s). At the present time, we have no sound explanation for this discrepancy. The absence of slow relaxation of magnetization for **3** is remarkable in view of the negative D values derived from the fittings of the dc magnetic data and from CASSCF/SOCI calculations.

The general difference between the ac magnetic behavior of the cobalt and iron compounds might, apart from the difference of the values of the spin−orbit coupling constant λ of the free ions (larger g-factor variation of the Co^{2+} complexes), also be explained by the fact that Co^{2+} is a noninteger spin system, a so-called Kramers ion.[14,50] Quantum tunneling by E is among others thought to be one of the reasons for lowering the theoretical spin reversal barrier. For every $S > 1/2$ the rhombic anisotropy parameter E mixes only the M_S ±2 states. Hence, the $\pm M_S$ components of the Kramers doublets can not be mixed by E. Although the other components can mix, for example, for an $S = 3/2$ ion the $M_S = +3/2$ state can mix with $M_S = -1/2$ and vice versa, these states are energetically separated by D (in terms of eq 1) which makes mixing of M_S states and thus quantum tunneling in Kramers ions less probable compared to non-Kramers ions. From Table 2 there seems to be a correlation in **1**−**6** between the lowering of the symmetry which is accompanied by the exchange of one strong σ-donor/π-donor −N(SiMe$_3$)$_2$ ligand against a σ-donor/weak π-donor THF ligand and a σ-donor/π-acceptor PCy_3 ligand on the one side, and the increase of the magnetic anisotropy expressed by the anisotropy of the g-factors and the D values on the other side. In addition, at a first glance one could also conclude that differences in magnetic anisotropy are mirrored by different sizes of the energy barrier for the relaxation of magnetization (although less pronounced for the cobalt complexes). However one has to consider that the observed energy barriers are by far smaller than the calculated ones ($U = S^2|D|$ for integer spin and $U = (S^2 - 0.25)|D|$ for half integer spin) which is a commonly observed phenomenon and usually assigned to the presence of quantum tunnelling effects.[10,14] It was also already pointed out that the ZFS parameters derived from fittings to eq 1 and from CASSCF/SOCI calculations on model complexes partially include contributions from strong spin−orbit coupling effects. Furthermore, as already indicated by the strong curvature of the ln τ versus $1/T$ graph it might be possible that the Arrhenius model cannot be reasonably applied here to fully describe the relaxation behavior of **1**−**6**. Other

dx.doi.org/10.1021/ic401677j | Inorg. Chem. 2014, 53, 1962−1974

mechanisms of spin interaction and spin relaxation might be also effective like recently shown.[1,6,7]

We rule out the presence of dominant intermolecular interactions because the shortest M···M distances are long and not very different (**1**: 894.0, **2**: 896.0, **3**: 873.7, **4**: 880.2, **5**: 923.7, **6**: 916.8 pm). In this respect it was found for $[Co(SPh)_4]^{2-}$ that mitigating intermolecular interaction by diluting the sample has only an influence on the quantum tunneling pathways (at low temperatures) whereas the value of the energy barrier U_{eff} remains unchanged.[14]

Theory. The interpretation of the magnetic data of **1** to **6** leaves some questions especially concerning the distinctly different behavior of **3** and **5** in the ac magnetic measurements. In addition we were primarily interested in the question whether the energy of the first transition may be used as rough estimate when estimating the size of the ZFS in **1**−**6** as outlined before.[16,35,51]

Electronic structures of compounds **1a**, **2a**, and **3**−**6** were calculated with density functional theory (DFT), and are shown in Figure 6 and Figures S29−S34 in the Supporting Information. Data presented below were obtained with the BP86 functional (and def2-TZVP bases), and the results are qualitatively the same for the B3LYP functional. We start with the discussion of the energetic sequence of the calculated minority spin (beta spin) frontier metal d orbitals (Figure 6).

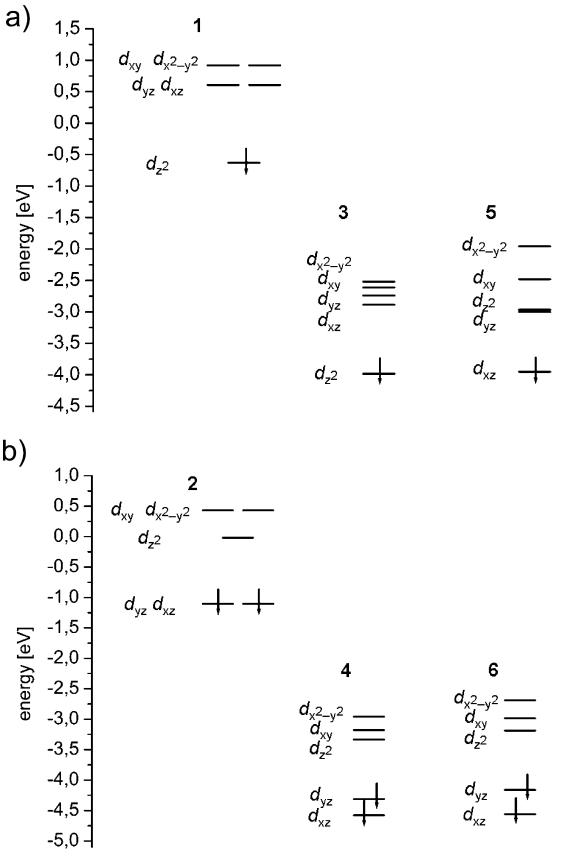

Figure 6. Energies and occupations of the five minority spin frontier orbitals of (a) $[Fe\{N(SiMe_3)_2\}_3]^-$ (**1a**), $[Fe\{N(SiMe_3)_2\}_2(THF)]$ (**3**), $[Fe\{N(SiMe_3)_2\}_2(PCy_3)]$ (**5**) and (b) $[Co(N(SiMe_3)_2)_3]^-$ (**2a**), $[Co(N(SiMe_3)_2)_2(THF)]$ (**4**), $[Co(N(SiMe_3)_2)_2(PCy_3)]$ (**6**) and the orientation of the metal d orbital contribution. The *z* axis is perpendicular to the trigonal plane, and the *x* axis points to the THF or PCy_3 ligand.

For **1a** and **3** it matches the qualitative orbital schemes derived from crystal field theory for an idealized trigonal-planar geometry (d^1 case) and the removal of degeneracy of the *e*-symmetry orbitals in the distorted structures (Figure S35 in the Supporting Information).[2,52] For **1a** and **3** the d_{z^2} orbital is lowest in energy and thus occupied. In **5** the d_{xz} orbital instead of the d_{z^2} is lowest in energy and occupied, being stabilized by the π-acceptor abilities of the PCy_3 ligand; this was also observed in reference 16. This change of electron density distribution from the axial position toward the trigonal plane may influence the magnetic anisotropy, which would be in line with the different ac magnetic properties of **5** in comparison with **1** and **3**.

For all three cobalt complexes **2a**, **4**, and **6** the d_{xz} and d_{yz} orbitals are lowest in energy and thus occupied. Highest in energy are d_{xy} and $d_{x^2-y^2}$, d_{z^2} is in between. Therefore the lowest orbitals are either energetic degenerate and equally populated (**2a**) or nondegenerate (**4**, **6**). Again, this order is contrary to the qualitative orbital schemes derived from crystal field theory which neglects electron−electron interactions (Figure S35 in the Supporting Information).[2,52] Because of these schemes, the degenerate d_{xz} and d_{xy} orbitals would be unequally populated in **2a** resulting in a Jahn−Teller distortion which is not evidenced by the calculated and measured structural parameters. Thus, in contrast to the iron complexes, the orbital sequence is the same for all cobalt complexes irrespective of the kind of ligands.

In all complexes **1a**, **2a**, and **3**−**6**, minority spin d orbitals are nondegenerate, leading to $L = 0$ for the ground states. Thus only mixing of excited states into the ground state by spin−orbit coupling can act as a main source of magnetic anisotropy expressed by the size of the ZFS. Within a perturbative approach, the magnitude of the coupling is proportional to the energetic accessibility of excited states.[37,53] Calculations of the electronic d−d transitions by time-dependent density functional theory (TDDFT) were performed on **1a**, **2a**, and **3**−**6** (Table 3). As expected, for compounds **1a**, **3**, and **5** and for compounds **2a**, **4**, and **6**, four and six d−d transitions, respectively, are obtained, which are partly degenerate in **1a** and **2a**. With the exception of compound **5** the positions of the peaks are quite well-reproduced in the experimental spectra as far as they are in the window of the experiment (see section Electronic Spectra and Figures S36−S40 and Tables S9−S14 in the Supporting Information).

The values for the lowest energy transition ΔE range from 0.19 to 0.35 eV (1533−2824 cm^{-1}) in **2a** and **3**−**6**, the value for **1a** is significantly higher, 0.66 eV (5324 cm^{-1}) (Table 3). The energy difference between the lowest energy transitions of trigonal-planar **1** and **5** amounts to 0.41 eV (3307 cm^{-1}) and is therefore comparable to those reported for **5** and the tetrahedral complex $[Fe\{N(SiMe_3)\}_2(dppe)]$ which display values of 0.39 eV (3146 cm^{-1}) or 0.44 (3549) from PBE or B3LYP calculations respectively.[16] Note that the excitation energies obtained by TDDFT, i.e. the poles of the response on an alternating field, are quite different from the energy differences of occupied and virtual ground state orbitals. The latter serve as a starting point, but large changes may happen within the TDDFT procedure, in particular, if exchange interactions are relevant. In view of the latter investigations which reveal that **5** behaves as a single-ion magnet whereas $[Fe\{N(SiMe_3)\}_2(dppe)]$ does not, these numbers may help to rationalize the distinctly smaller influences of ZFS (no out-of-phase ac signal) for **1** compared to **5**, but not the different magnetic behavior of **3** and **5**, for which the energy of the first

dx.doi.org/10.1021/ic401677j | Inorg. Chem. 2014, 53, 1962−1974

Table 3. Calculated (TDDFT) and Experimentally Observed d−d Transition Energies ΔE in 1−6[a]

$[Fe\{N(SiMe_3)_2\}_3]^-$ (1a)				$[Fe\{N(SiMe_3)_2\}_2(THF)]$ (3)				$[Fe\{N(SiMe_3)_2\}_2(PCy_3)]$ (5)			
theory		experiment		theory		experiment		theory		experiment	
ΔE	f	ΔE	ε	ΔE	f	ΔE	ε	ΔE	f	ΔE	ε
1.43	1.23	1.31	100	1.33	1.11	1.25	17	1.71	0.69	1.33	25
1.43	1.23			1.28	1.04	1.07	27	1.29	0.05	1.03	32
0.66	0.05			0.81	0.04			0.68	0.31		
0.66	0.05			0.29	0.02			0.25	0.02		
$[Co\{N(SiMe_3)_2\}_3]^-$ (2a)				$[Co\{N(SiMe_3)_2\}_2(THF)]$ (4)				$[Co\{N(SiMe_3)_2\}_2(PCy_3)]$ (6)			
theory		experiment		theory		experiment		theory		experiment	
ΔE	f	ΔE	ε	ΔE	f	ΔE	ε	ΔE	f	ΔE	ε
1.69	2.9	1.78	155	1.59	3.4	1.83	105	1.87	1.11	1.89	61
1.69	2.9			1.46	0.006			1.69	0.32	1.7	90
1.15	0	0.92	20	1.06	0.004	0.81	10	1.14	0.07	0.98	19
1.04	0.34			0.93	0.16			0.99	0.43	0.85	28
0.19	0.0003			0.52	0.007			0.58	0.03		
0.19	0.0003			0.35	0.13			0.19	0.05		

[a]Parameters: transition energy ΔE [eV], corresponding oscillator strength f (multiplied by 10^3) and extinction coefficient(ε [l mol^{-1} cm^{-1}]). For the spectra, see Figures S30−S35 in the Supporting Information, and for an assignment of the d−d transitions see Tables S9−S14 in the Supporting Information.

transition is very similar. Obviously the above estimation, which is considering only the energy denominator of the first term in the perturbative expansion for the spin−orbit coupling, is not sufficient here, probably, as the electronic situation (orientation of occupied d-orbitals) in **5** is very different from that in **3**. Improvement may be achieved by regarding also subsequent terms arising from higher transitions as well as finding suitable weights for each term.

For the three cobalt complexes, the calculated lowest d−d excitation energies are quite similar among each other (unlike for the iron compounds). They amount to 0.19 eV (1533 cm^{-1}) for **2a**, to 0.35 eV (2823 cm^{-1}) for **4**, and to 0.19 eV (1533 cm^{-1}) for **6**. This similarity is in line with similar g parameters, relaxation times and energy barriers (Table 2) for compounds **2**, **4**, and **6** and a moderate variance of the anisotropy parameters D and E derived from the experimental data (see Table 2).

DFT calculations of D and E in the way proposed by Neese and co-workers[54,55] yield similar values for all compounds of the respective metal. For the iron complexes, calculated D values ranges from −3.7 to −2.7 cm^{-1}, whereas for the cobalt compounds from +10.6 to +11.3 cm^{-1}; calculated values of E/D ranges from 0.21 to 0.23 for the iron compounds and from 0.05 to 0.07 for the cobalt compounds. This discrepancy to the experimental data is not unexpected. A systematic computational study of high-spin Co(II)S_4-containing complexes already revealed that ab initio multireference wave function methods are superior to DFT computational methods when applied to calculate D values in a wider range than $-10 < D < +10$ cm^{-1}.[56]

We therefore performed complete active space self-consistent field (CASSCF) and spin−orbit configuration interaction (SOCI) calculations on model complexes of **1a**, **2a**, and **3**−**6** (see Experimental Section). The spin−orbit coupling contribution to the ZFS tensor is calculated by means of quasi-degenerate perturbation theory and effective Hamiltonian theory.[57] The results are summarized in Table 4 together with the first CASSCF excitation energies, and contributions of the CASSCF ground state to the lowest SOCI eigenvector. For a comparison of the experimentally determined and calculated

Table 4. Calculated (CASSCF) Lowest Transition Energies ΔE, Contributions of the CASSCF $^{2S+1}$A Ground State (Co: $S = 3/2$, Fe: $S = 2$) to the Lowest SOCI Eigenvector, ZFS Parameters D, and E/D of the Model Complexes 1−6

	ΔE [cm^{-1}/eV][a]	contrib. [%]	D [cm^{-1}][b]	E/D
$[Co(NH_2)_3]^-$	504.3/0.06	69.6	±97.5[c]	0.25
$[Co(NH_2)_2(OH_2)]$	1196.8/0.15	83.5	±77.1[c]	0.32
$[Co(NH_2)_2(PH_3)]$	1489.3/0.19	87.3	±71.8[c]	0.28
$[Fe(NH_2)_3]^-$	2539.4/0.32	97.5	+12.3	0.01
$[Fe(NH_2)_2(OH_2)]$	80.8/0.01	55.4	−75.9	0.01
$[Fe(NH_2)_2(PH_3)]$	477.9/0.06	75.2	−53.2	0.01

[a]Lowest transition energies obtained from CASSCF naturally differ from those derived by TDDFT (Table 3). However, these transitions could not be detected due to experimental limitations. [b]The meaning of the D parameter in terms of eq 1 becomes unreliable in the case of strong contributions of excited determinants. [c]The sign of calculated D becomes ambiguous in the limit of extreme rhombicity ($E/D \rightarrow 1/3$).

ZFS parameters (Tables 2 and 4) one has to consider that in the case of distinct admixtures of excited states, the calculated ZFS parameters will loose their original physical meaning. In addition, it is known that in the case of large rhombicity ($E/D \rightarrow 1/3$), as obtained for all three cobalt complexes, the sign of the calculated D is vague.[58] It was also already mentioned above that strong spin−orbit coupling contributions, whenever present, are not considered by the Hamiltonian (eq 1) used in the fittings. In agreement with this the discrepancies between calculated and experimentally derived D values are found to be pronounced in **2**/**2a**, **3**, and **5** with strong admixtures of excited determinants (>20%) and lowest energy transitions below 500 cm^{-1}. In contrast calculated D values of the model complexes of **1a** (+12.3 cm^{-1}), **4** (±77.1 cm^{-1}), and **6** (±71.8 cm^{-1}) are in good agreement with the experimental ones (**1**: +9.9 cm^{-1}, **4**: −72 cm^{-1}, **6**: −82 cm^{-1}), in line with admixtures of excited determinants less than 20% and lowest energy transitions above 1000 cm^{-1}.

Electronic Spectra. Electronic spectra of compounds **1**−**6** were measured in a region from 5.8 to 0.56 eV (46 800−4520 cm^{-1}), with the compounds in THF solution and as polycrystalline powders between two quartz plates, and they

dx.doi.org/10.1021/ic401677j | Inorg. Chem. 2014, 53, 1962−1974

were compared with the transitions calculated by TDDFT (Table 3, Figures S36–S40, Tables S9–S14 in the Supporting Information). Because of the occurrence of sharp bands, which we assign to vibration overtones, the spectra were not recorded further into the infrared (IR) region. In view of the extinction coefficients of the bands in solution (ε > 2000 and ε < 150 l mol^{-1} cm^{-1}) all spectra can be roughly divided into a region above and below 2.5 eV (20 165 cm^{-1}), the former ones assigned to charge transfer bands and the latter ones belonging to d–d transitions. The position and appearance of the charge-transfer bands differ for the same compound measured in solution and in the solid state, which could be attributed to solvatochromic effects and the nonvalidity of Lambert–Beers law for the crystal mulls. However, the positions of these bands correspond to the region observed for the d^0 metal-ion complex [Sc{N(SiMe$_3$)$_2$}$_3$] (5.06 eV (40 814 cm^{-1}) and 3.86 eV (31 135 cm^{-1}))[59] and the trivalent cobalt and iron analogues [M{N(SiMe$_3$)$_2$}$_3$] (M = Co: 4.63 eV (37 346 cm^{-1}) and 3.90 eV (31 457 cm^{-1}),[60] M = Fe 3.68 eV (29 683 cm^{-1}), 3.14 eV (25 324 cm^{-1}))[59].

For a free Fe^{2+} ion the ground state is ^{5}D$_4$, which in a trigonal-planar crystal field of D_{3h} point-group symmetry splits into ^{5}A′ + ^{5}E′ + ^{5}E″, whereas the ^{4}F$_{9/2}$ ground state of a free Co^{2+} ion would split in the same field into ^{4}A′ + (^{4}A$_1$″, ^{4}A$_2$″) + ^{4}E′ + ^{4}E″.[59] In the ideal symmetric complexes one would therefore expect two d–d transitions for the iron and three d–d transitions for the cobalt complexes. Lowering of the symmetry should affect a splitting of the degenerated states, leading to four transitions in the iron case and six for the cobalt complexes.

In the region from 2.5 to 0.56 eV (20 165–4520 cm^{-1}) we observed for the iron complexes **1**, **3**, and **5** in principle one band around 1.15 eV (9276 cm^{-1}), which is split upon lowering the symmetry. As the solution spectra of **5** in THF are due to quick ligand exchange almost the same as that of **3** (not shown), we remeasured **5** in toluene.

For the cobalt complexes **2**, **4**, and **6**, we observe in the same spectral region two bands around 1.8 eV (14 520 cm^{-1}) and 0.85 eV (6856 cm^{-1}). Splitting of the bands is only observed in the case of the solid-state spectrum of **6**. The bright-green color of the cobalt complexes can therefore be attributed to the d–d transitions around 1.8 eV (14520 cm^{-1}), whereas the slight differences in the pale colors of the iron compounds are determined by the different onsets of the charge transfer bands.

A comparison of the experimental spectra with the calculated d–d transitions (Table 3) has to take into account that the differences in the position of the bands could originate from the difference in temperature between measurements and calculations. In addition the experimental intensities and thus the possibility of observing the transitions could also depend on temperature as well as the sample environment (crystal lattice or solution). For the cobalt complexes **2**, **4**, and **6** the agreement between theory and experiment is in general quite good, suggesting that the lowest-energy transitions are located further down in the IR region, which makes them difficult to detect due to the appearance of vibration modes of the ligands. For the iron complexes we found a good match for the spectra of **1** and **3**, while that of **5** does not agree with the predicted one. This might indicate that, upon cooling, the electron distribution and orbital sequence of **5** distinctly changes. However, also in the case of the iron complexes, the lowest-energy transitions are to be found below 0.5 eV (4033 cm^{-1}) or are too low in intensity, according to small calculated values of the oscillator strength.

Information about d–d transitions in the absorption spectra of comparable bis(trimethylsilyl)amido compounds of iron and cobalt, especially in the formal oxidation state 2+ in the literature, are scarce. For the trivalent complexes [M{N(SiMe$_3$)$_2$}$_3$] (M = Fe, Co), transitions have been reported at 2.0 eV (16 132 cm^{-1}) and 2.48 eV (20 004 cm^{-1}) for the iron compound,[59] while the cobalt analogue was found to show two absorptions at 2.73 eV (22 020 cm^{-1}) and 2.07 eV (16 697 cm^{-1}).[60] Intensities were found to be quite strong in the both cases ([Fe{N(SiMe$_3$)$_2$}$_3$]: $\varepsilon \approx$ 400–450 l mol^{-1} cm^{-1}; [Co{N(SiMe$_3$)$_2$}$_3$]: $\varepsilon \approx$ 2900–3600 l mol^{-1} cm^{-1}). For the four- and three-coordinated Co^{2+} complexes [Co{N(SiMe$_3$)$_2$}$_2$(py)$_2$] and [Co{N(SiMe$_3$)$_2$}$_2$(py)], two narrow bands around 1.91 eV (15 406 cm^{-1}) and 1.78 eV (14 358 cm^{-1}) with $\varepsilon \approx$ 300–350 l mol^{-1} cm^{-1} were observed quite similar to the transitions we have found.[22] Absorption bands further in the near-IR have so far not been reported.[30] However, it is known that in four-coordinate tetrahedral and pseudotetrahedral cobalt(II) and iron(II) complexes the ^{4}T$_1$(F)←^{4}A$_2$ and ^{5}T$_2$←^{5}E transitions, respectively, appear as broad absorptions in the near-IR.[61]

Mößbauer Spectra. ^{57}Fe Mößbauer spectra of all three compounds **1**, **3**, and **5** at 3 K and at higher temperatures exhibit a doublet (Figures S42–S45 in the Supporting Information). This behavior is characteristic of an integer spin paramagnet. Small values of the isomer shifts (δ) of 0.59 (**1**), 0.57 (**3**), and 0.59 mm/s (**5**) at 3 K are comparable with other values found for high-spin three-coordinated iron(II) ions in a weak ligand field (Supporting Information, Table S15).[2,62–64] Similar δ values for all three compounds indicate a negligible influence of the different bonding situations in **1**, **3**, and **5** on the s electron density at the iron nuclei. The observed decrease in the isomer shifts of all compounds with increasing temperature (Figures S42–S44 in the Supporting Information) results from a second-order Doppler-shift contribution. Contrary to the isomer shifts, the quadrupole splitting values of 0.60 (**1**), 1.86 (**3**), and 1.25 mm/s (**5**) at 3 K are very different. The formal oxidation state +II and the spin state (high-spin) is assumed to be similar for all three complexes, as indicated by the results from single crystal XRD, magnetic measurements, and quantum-chemical calculations. Therefore the differences in the electric field gradient should mainly arise from different valence-electron contributions due to the different ligands and different degrees of distortion of the ligand field environment. The unusual small ΔE_Q value of compound **1**, which is in principle comparable to those of high-spin Fe(III)-S/SR complexes, is similar to that found in trigonal-planar [Fe(SC$_6$H$_3$-2,4,6-*t*-Bu$_3$)$_3$]$^-$ (ΔE_Q = 0.81 mm/s).[62] Upon lowering the symmetry in **3** and **5** compared to **1** the symmetric electron configuration (A′)^2(E″)^2(E′)^2, which is thought to be consistent with a relatively small quadrupole splitting,[60] changes, and ΔE_Q increases. In agreement with this, similar large values of ΔE_Q (1.74 −1.61 mm/s) were also observed before for the two unsymmetrically coordinated trigonal-planar complexes [(β-ketiminate) Fe(R)] (R = −CH$_3$, Cl$^-$).[2]

As is revealed in Figures S43–S45 in the Supporting Information, at temperatures between 144 and 3 K the quadrupole splittings are slightly dependent on temperature. For compound **1** the change is of 0.07 mm/s from 120 to 3 K; for **2**, it is 0.04 mm/s from 100 to 3 K, and for **3** it is −0.06

dx.doi.org/10.1021/ic401677j | Inorg. Chem. 2014, 53, 1962–1974

mm/s from 144 to 3 K. Changes in ΔE_Q with temperature are not unexpected in complexes of the type studied here, as a result of rearrangement in the thermal population of the large number of spin−orbit states.

CONCLUSION

The comparative experimental and theoretical study of the physical properties of the two sets of trigonal-planar M = Fe^{2+}, Co^{2+} high-spin complexes [Li(15-crown-5)] [M{$N(SiMe_3)_2$}$_3$], [M{$N(SiMe_3)_2$ }$_2$(THF)], and [M{$N(SiMe_3)_2$ }$_2$(PCy_3)] leads to the following conclusions.

Single-crystal X-ray diffraction analysis suggests only small deviations (<3.0 pm) from trigonal planarity for the metal atoms in all six complexes. In agreement with considerable magnetic anisotropy derived from the dc magnetic data, the Co^{2+} complexes display slow relaxation of the magnetization at low temperatures; whereas, in the case of the iron compounds, only [Fe{$N(SiMe_3)_2$}$_2$ (PCy_3)] comprises sufficiently high anisotropy to show a similar behavior in the ac magnetic measurements. The energetic ordering of the minority spin frontier orbitals reveals that L = 0 for the ground states of all complexes. Thus only mixing of excited states into the ground state by spin−orbit coupling can act as a main source of magnetic anisotropy, as is indicated to be present in all compounds except [Li(15-crown-5)] [Fe{$N(SiMe_3)_2$}$_3$] by CASSCF/SOCI calculations on model complexes. To relate the different behavior of the complexes in the ac measurements to the ZFS parameters derived either from fits to a spin Hamiltonian or from CASSCF/SOCI calculations on model complexes, one has to be careful for two reasons. The absolute value of D derived from CASSCF/SOCI calculations loses its original meaning in the case of strong contributions of excited determinants. In addition strong mixing with excited states suggests the presence of orbital momentum contributions, which are not considered by the Hamiltonian used in the fittings of the dc magnetic data. In general the different behavior of the two sets of complexes in the dc and ac magnetic measurements is in agreement with a stronger spin−orbit coupling constant λ of the free Co^{2+} ion in comparison with Fe^{2+}. In addition Co^{2+} is a so-called Kramers ion in which mixing of the ground $\pm M_S$ levels by transverse ZFS E is forbidden, which leads to a minimization of the probability of quantum tunneling.

The special magnetic behavior of [Fe{$N(SiMe_3)_2$}$_2$ (PCy_3)] among the three iron complexes correlates with a change in the local magnetic anisotropy. DFT calculations reveal for this complex a change of the energetic order and occupation of the d_{z^2} and the d_{xz}/d_{yz} minority spin frontier orbitals upon coordination of the σ-donor/π-acceptor PCy_3 ligand. This differs from the prediction by crystal-field theory, for which d_{z^2} is lowest in energy as observed in the other two iron complexes. In contrast, the absence of a spin-reversal barrier in [Li(15-crown-5)] [Fe{$N(SiMe_3)_2$}$_3$] is in line with a positive D (confirmed by CASSCF/SOCI calculations and also indicated by Mößbauer spectroscopy) and the highest calculated energy for the lowest transition by TDDFT and CASSCF/SOCI.

In case of the cobalt compounds, for all three complexes, the d_{xz}/d_{yz} minority spin frontier orbitals are occupied. Exchanging the strong σ-donor/π-donor −$N(SiMe_3)_2$ ligand against one σ-donor/weak π-donor THF ligand or a σ-donor/π-acceptor PCy_3 ligand has only a moderate influence on the orbital energies and does not change their sequence. The energy barriers of the cobalt complexes differ only slightly, which is in line with modest variances in the anisotropy parameters and lowest energy differences. However, one has to remember that, for the determination of the effective energy barriers, probably more influential parameters like spin-reversal relaxation pathways other than an Orbach process also have to be taken into consideration, as was recently outlined for example by Atanosov et al.[7] In addition, to obtain a more refined picture of the magnetic properties of the complexes under investigation, one would also have to confirm the obtained anisotropic g values and the sign and size of the D values by high-field electron spin resonance and magnetic measurements on single crystals.

EXPERIMENTAL SECTION

Synthesis. Standard Schlenk techniques were employed throughout the syntheses using a double manifold vacuum line with high-purity dry nitrogen (99.9994%) and an MBraun Glovebox with high-purity dry argon (99.9990%). The solvent THF (tetrahydofuran) and toluene were dried over sodium benzophenone, *n*-heptane over $LiAlH_4$, and distilled under nitrogen. Anhydrous dimethylenechloride (CH_2Cl_2) (H_2O < 0.005%) obtained from Aldrich was degassed, freshly distilled, and stored over molecular sieves under nitrogen. $LiN(SiMe_3)_2$, PCy_3 (Cy = cyclohexyl, C_6H_{11}), and anhydrous $CoCl_2$ were purchased from Aldrich. $LiN(SiMe_3)_2$ was distilled prior to use. [Fe{$N(SiMe_3)_2$}$_2$]$_2$[19] and [Co{$N(SiMe_3)_2$}$_2$]$_2$[17] were synthesized according to literature procedures.

*[Li(15-crown-5)][Fe{$N(SiMe_3)_2$}$_3$] (**1**).* [Fe{$N(SiMe_3)_2$}$_2$]$_2$ (0.25 g, 0.332 mmol) and Li $N(SiMe_3)_2$ (0.111 g, 0.664 mmol) were dissolved in 10 mL of toluene. Addition of 15-crown-5 (0.13 mL, 0.664 mmol) resulted in the formation of a heavier green phase and a lighter colorless phase. When it is cooled to approximately −70 °C by a dry ice/methanol bath, the green phase becomes highly viscous. The supernatant solution was replaced by 10 mL of toluene, warmed up, stirred for a few minutes, and cooled again. After removal of the lighter phase the rest was warmed to room temperature again and dried in vacuum to give a dirty-green residue, which was redissolved in 5 mL of CH_2Cl_2. Addition of 4.5 mL of *n*-heptane led to the formation of crystals upon standing in the refrigerator (−42 °C). Another 5 mL of *n*-heptane were added to complete the crystallization, and then the whole solvent was removed at low temperatures before the crystals were washed two times with heptane at room temperature to give a total yield of 0.36 g (71%) of **1**.

Anal. Calcd for $C_{28}H_{74}O_5FeLiN_3Si_6$ (764.21): C 44.0, H 9.8, N 5.5. Found: C 43.6, H 9.8, N 5.6%.

When it is heated, **1** decomposes visibly above 190 °C.

[Li(15-crown-5)] [Co{$N(SiMe_3)_2$}$_3$] (**2**) was prepared in a similar procedure to that of compound **1** from 0.25 g (0.332 mmol) of [Co{$N(SiMe_3)_2$}$_2$]$_2$ and equimolar amounts of $LiN(SiMe_3)_2$ and 15-crown-5 to yield 0.33 g (65%) of **2**.

Anal. Calcd for $C_{28}H_{74}O_5CoLiN_3Si_6$ (767.30): C 43.8, H 9.7, N 5.5. Found: C 44.9, H 9.8, N 5.3%. A slightly enhanced value for C and simultaneous decrease of N could be explained by traces of CH_2Cl_2 in the crystalline powders.

When it is heated, **2** decomposes visibly above 170 °C.

*[Fe{$N(SiMe_3)_2$}$_2$(THF)] (**3**).* Addition of 1 mL of THF to [Fe{$N(SiMe_3)_2$}$_2$]$_2$ (2 g, 2.66 mmol) resulted, after gentle heating, in the formation of a dark-green solution. Slow removal of excess THF under reduced pressure afforded pale-green crystals of **3** with a total yield of 2.3 g (97%).

Anal. Calcd for $C_{16}H_{44}OFeN_2Si_4$ (448.73): C 42.8, H 9.9, N 6.2. Found: C 42.5, H 10.1, N 6.2%.

Crystals of **3** melt at around 45 °C and are extremely air- and moisture-sensitive. Visible decomposition results in a quick color change and formation of a black oil.

*[Co{$N(SiMe_3)_2$}$_2$(THF)] (**4**).* Addition of 1 mL of THF to [Co{$N(SiMe_3)_2$}$_2$]$_2$ (2 g, 2.63 mmol) resulted, after gentle heating, in the formation of a dark-green solution. Slow removal of excess THF under

dx.doi.org/10.1021/ic401677j | Inorg. Chem. 2014, 53, 1962−1974

reduced pressure afforded intensely green crystals of **4**, with a total yield of 2.3 g (96%).

Anal. Calcd for $C_{16}H_{44}OCoN_2Si_4$ (451.81): C 42.5, H 9.8, N 6.2. Found: C 41.9, H 9.8, N 6.1%.

Crystals of **4** melt at around 75 °C and are extremely air- and moisture-sensitive. Visible decomposition results in a quick color change from original intense green to black.

*[Fe{N(SiMe$_3$)$_2$}$_2$(PCy$_3$)] (**5**).* $[Fe\{N(SiMe_3)_2\}_2]_2$ (0.5 g, 0.66 mmol) and PCy_3 (0.37 g, 1.34 mmol) were dissolved in 5 mL of heptane; when the mixture was gently heated, a dark brown solution resulted. Evaporation of half of the solvent afforded the formation of a pale powder that dissolves upon gentle heating to give **5** as huge pale-green crystals after it stands in the freezer (−40 °C) for 3 d. These crystals were washed two times with cold (−60 °C) pentane and dried under vacuum to give a total yield of 0.53g (61%).

Anal. Calcd for $C_{30}H_{69}FeN_3PSi_6$ (657.05): C 54.8, H 10.6, N 4.3. Found: C 54.9, H 10.6, N 4.3%.

*[Co{N(SiMe$_3$)$_2$}$_2$(PCy$_3$)] (**6**).* $[Co\{N(SiMe_3)_2\}_2]_2$ (1 g, 1.33 mmol) and PCy_3 (0.74 g, 2.66 mmol) were dissolved in 10 mL of heptane; when the mixture was gently heated, a dark green solution resulted. Evaporation of half of the solvent afforded the formation of a pale powder that dissolves upon gentle heating to give **6** as green crystals after it stands in the freezer (−40 °C) for 3 d. These crystals were washed two times with cold (−60 °C) pentane and dried under vacuum to give a total yield of 1.2 g (68%).

Anal. Calcd for $C_{30}H_{69}CoN_3PSi_6$ (660.14): C 54.6, H 10.5, N 4.2. Found: C 54.6, H 10.6, N 4.1%.

Crystallography. Because of the extreme air and moisture sensitivity of the compounds, crystals suitable for single-crystal X-ray diffraction were selected in perfluoroalkylether oil in a glovebox and transferred rapidly under argon atmosphere to the diffractometer equipped with an Oxford Cryosystem. Single-crystal X-ray diffraction data of **1**, **2**, **4**, and **6** were collected using graphite-monochromatised Mo Kα radiation (λ = 0.710 73 Å) on a STOE IPDS II (imaging plate diffraction system). Raw intensity data were collected and treated with the STOE X-Area software Version 1.39. Data for all compounds were corrected for Lorentz and polarization effects.

On the basis of a crystal description, a numerical absorption correction was applied for **4.**[65] The structures were solved with the direct methods program SHELXS of the SHELXTL PC suite of programs[66] and were refined with the use of the full-matrix least-squares program SHELXL. Molecular diagrams were prepared using Diamond.[67]

In **1**, **2**, **3**, and **6** all Fe, Co, Si, N, and C atoms were refined with anisotropic displacement parameters, while H atoms were placed in fixed positions. In **1** and **2**, solvent CH_2Cl_2 molecules and parts of the 15-crown-5 ether molecules were refined with a split model of site disorder. In **4** the C atoms (C(1), C(3), C(4), and C(6)) were refined with a split model of site disorder.

CCDC-873291 (**1**), 873292 (**2**), 863806 (**4**), and 884241 (**6**) contain the supplementary crystallographic data for this Paper. These data can be obtained free of charge at www.ccdc.cam.ac.uk/conts/retrieving.html (or from the Cambridge Crystallographic Data Centre, 12 Union Road, Cambridge CB2 1EZ, UK; fax: (internat.) +44−1223/336−033; e-mail: deposit@ccdc.cam.ac.uk).

X-ray powder diffraction patterns (XRD) for **1** and **2** (suspension of crystals in CH_2Cl_2) and **3**−**6** (powder of crystals) were measured on a STOE STADI P diffractometer (Cu Kα_1 radiation, Germanium monochromator, Debye−Scherrer geometry, Mythen 1K detector) in sealed glass capillaries. The theoretical powder diffraction patterns were calculated on the basis of the atom coordinates obtained from single-crystal X-ray analysis by using the program package STOE WinXPOW.[68]

Physical Measurements. C, H, and N elemental analyses were performed on an Elementar vario Micro cube instrument.

The ultraviolet−visible absorption spectra in THF (**1**−**4**) and toluene (**5**, **6**) were measured on a Perkin-Elmer Lambda 900 spectrophotometer in quartz cuvettes. Solid-state spectra were measured in transmission as micrometer-sized crystalline powders between quartz plates in front of a Labsphere integrating sphere.

Zero-field-cooled temperature-dependent susceptibilities were recorded for **1**−**6** in dc mode using a MPMS-5S (Quantum Design) SQUID magnetometer over a temperature range from 2 to 300 K in a homogeneous 0.1 T external magnetic field. The ac susceptibility measurements were performed with an oscillating ac field of 3 Oe and ac frequencies ranging from 1 to 1500 Hz. The magnetization curves were measured on the same instrument up to a dc field of 5 T. The samples were contained in gelatin capsules filled in a glovebox under argon atmosphere, owing to the high degree of moisture and oxygen sensitivity of the compounds. The samples were transferred in sealed Schlenk tubes from the glovebox to the magnetometer and then rapidly transferred to the helium-purged sample space of the magnetometer. The data were corrected for the sample holder including the gelatin capsule and for diamagnetism using Pascal's constants.[69−71] Details about the simulations are given in the Supporting Information.

The Mößbauer spectra were acquired using a conventional spectrometer in the constant-acceleration mode equipped with a ^{57}Co source (3.7 GBq) in rhodium matrix. Isomer shifts are given relative to α-Fe at room temperature. The samples were pressed in a homemade holder between two 0.075 mm thick polyimide foils (covered on the sample side with a 300 nm Al layer) separated by a Viton O-ring inside a glovebox and then inserted inside an Oxford Instruments Mößbauer-Spectromag 4000 Cryostat. The sample temperature can be varied between 3.0 and 300 K. Three Kelvin temperature could be achieved by pumping the sample space.

Quantumchemical Calculations. Density functional calculations for complexes **1**−**6** were carried out with the program system TURBOMOLE[72] for the ground state[73,74] as well as for the excited states,[75] using functionals BP86[76,77] and B3LYP,[78] def2-TZVP[79] basis sets, and corresponding RI-J auxiliary basis sets.[80]

The CASSCF and SOCI calculations on the model complexes of **1** and **2** were performed using the ORCA program package in version 3.0.0.[55] The X-ray geometries were truncated to $[M(NH_2)_3]^-$, $[M(NH_2)_2(OH_2)]$, and $[M(NH_2)_2(PH_3)]$ (M = Fe, Co) (Tables S16 and S17 in the Supporting Information). After replacing the functional groups with their simplified derivatives, only the coordinates of the hydrogen atoms were optimized at the DFT level of theory using the TURBOMOLE[72] program system employing the B3LYP[78] functional. In all calculations def2-TZVPP[79] basis sets were used. Molecular orbitals were determined for the average of the 10 and 5 high-spin roots at the CASSCF level of theory, choosing the five 3d-based orbitals of Fe and Co as active, giving rise to CAS(6,5) and CAS(7,5). The spin−orbit coupling matrix was constructed within the active space and diagonalized to give the ZFS parameters, using effective Hamiltonian theory.[57] In test calculations, the spin−spin coupling contributions to the ZFS tensor are below 1 cm^{-1}.

■ ASSOCIATED CONTENT

Supporting Information

Equations 1−6 for the simulation of the dc and ac magnetic data. Tables S1−S17 for the relaxation fitting parameters from least-squares fitting and Cole−Cole plots for χ'' versus χ', calculated and experimentally observed d−d transitions, Mößbauer parameters for three-coordinate Fe^{2+} complexes, Cartesian coordinates of model complexes from the CASSCF calculations. Figures S1−S45 for the molecular structure of the cation $[Li_2(15\text{-crown-}5)_2]^{2+}$ (**1b**), measured and simulated X−ray powder patterns, field dependence of the magnetization **M** at 2 K, plots of magnetization **M** versus *H* measured between 2 and 6 K and the corresponding fittings, frequency dependence of χ' and χ'' at 2 K under different dc fields, temperature dependence χ' and χ'' under a given dc field at different frequencies, frequency dependence of χ' and χ'' under a given dc field at different temperatures, Cole−Cole plots for χ'' versus χ', contour plots of the calculated minority spin d orbitals ordered by their orbital energies, schematic 3d orbital level

dx.doi.org/10.1021/ic401677j | Inorg. Chem. 2014, 53, 1962−1974

schemes, comparison of the experimental electronic spectra as a powder of crystals between quartz plates and in THF with the d−d transitions calculated by TDDFT, zero-field Mößbauer spectra at different temperatures. This material is available free of charge via the Internet at http://pubs.acs.org. CCDC-873291 (**1**), 873292 (**2**), 863806 (**4**), and 884241 (**6**) contain the supplementary crystallographic data for this Paper. These data can be obtained free of charge at www.ccdc.cam.ac.uk/conts/retrieving.html (or from the Cambridge Crystallographic Data Centre, 12 Union Road, Cambridge CB2 1EZ, UK; fax: (internat.) +44−1223/336−033; e-mail: deposit@ccdc.cam.ac.uk).

AUTHOR INFORMATION

Corresponding Author

*E-mail: andreas.eichhoefer@kit.edu. Phone: 49-(0)721-608-26371. Fax: 49-(0)721-608-26368.

Notes

The authors declare no competing financial interest.

ACKNOWLEDGMENTS

This work was supported by the Karlsruhe Institut für Technologie (KIT, Campus Nord). The authors wish to thank A. K. Powell for generous support, K. Fink for helpful discussions concerning the calculation of ZFS parameters, and S. Stahl for the performance of the elemental analysis. T. Bodenstein acknowledges funding from Deutsche Forschungsgemeinschaft via SFB/TRR 88 "3MET".

REFERENCES

(1) Zadrozny, J. M.; Xiao, D. J.; Atanasov, M.; Long, G. J.; Grandjean, F.; Neese, F.; Long, J. R. *Nat. Chem.* **2013**, 577.

(2) Andres, H.; Bominaar, E. L.; Smith, J. M.; Eckert, N. A.; Holland, P. L.; Münck, E. *J. Am. Chem. Soc.* **2002**, *124*, 3012.

(3) Reiff, W. M.; LaPointe, A. M.; Witten, E. H. *J. Am. Chem. Soc.* **2004**, *126*, 10206.

(4) Reiff, W. M.; Schulz, C. E.; Whangbo, M.-H.; Seo, J. I.; Lee, Y. S.; Potratz, G. R.; Spicer, C. W.; Girolami, G. S. *J. Am. Chem. Soc.* **2009**, *131*, 404.

(5) Merill, W. A.; Stich, T. A.; Brynda, M.; Yeagle, G. J.; Fettinger, J. C.; de Hont, R.; Reiff, W. M.; Schulz, C. E.; Britt, R. D.; Power, P. P. *J. Am. Chem. Soc.* **2009**, *131*, 12693.

(6) Zadrozny, J. M.; Atanasov, M.; Bryan, A. M.; Lin, C.-Y.; Rekken, B. D.; Power, P. P.; Neese, F.; Long, J. R. *Chem. Sci* **2013**, *4*, 125.

(7) Atanasov, M.; Zadrozny; Long, J. R.; Neese, F. *Chem. Sci* **2013**, *4*, 139.

(8) Ishikawa, N.; Sugita, M.; Ishikawa, T.; Koshihara, S.; Kaizu, Y. *J. Am. Chem. Soc.* **2003**, *125*, 8694.

(9) Woodruff, D. N.; Winpenny, R. E. P.; Layfield, R. A. *Chem. Rev.* **2013**, *113*, 5110.

(10) Freedman, D. E.; Harman, W. H.; Harris, T. D.; Long, G. J.; Chang, C. J.; Long, J. R. *J. Am. Chem. Soc.* **2010**, *132*, 1224.

(11) Harman, W. H.; Harris, T. D.; Freedman, D. E.; Fong, H.; Chang, A.; Rinehart, J. D.; Ozarowski, A.; Sougrati, M. T.; Grandjean, F.; Long, G. J.; Long, J. R.; Chang, C. J. *J. Am. Chem. Soc.* **2010**, *132*, 18115.

(12) Weismann, D.; Sun, Y.; Lan, Y.; Wolmershäuser, G.; Powell, A. K.; Sitzmann, H. *Chem.—Eur. J.* **2011**, *17*, 4700.

(13) Jurca, T.; Farghal, A.; Lin, P.-H.; Korobkov, I.; Murugesu, M.; Richeson, D. S. *J. Am. Chem. Soc.* **2011**, *133*, 15814.

(14) Zadrozny, J. M.; Long, J. R. *J. Am. Chem. Soc.* **2011**, *138*, 20732.

(15) Zadrozny, J. M.; Liu, J.; Piro, N. A.; Chang, C. J.; Hill, S.; Long, J. R. *Chem. Commun.* **2012**, *48*, 3897.

(16) Lin, P.-H.; Smythe, N. C.; Gorelsky, S. I.; Maguire, S.; Henson, N. J.; Korobkov, I.; Scott, B. L.; Gordon, J. C.; Baker, R. T.; Murugesu, M. *J. Am. Chem. Soc.* **2011**, *135*, 15806.

(17) Bürger, H.; Wannagat, U. *Monatsh. Chem.* **1963**, *94*, 1007.

(18) Murray, B. D.; Power, P. P. *Inorg. Chem.* **1984**, *23*, 4584.

(19) Andersen, R. A.; Faegri, K.; Green, J. C.; Haaland, A.; Lappert, M. F.; Leung, A.-P.; Rypdal, K. *Inorg. Chem.* **1988**, *27*, 1782.

(20) Olmstead, M. M.; Power, P. P.; Shoner, S. C. *Inorg. Chem.* **1991**, *30*, 2547.

(21) Bradley, D. C.; Hursthouse, M. B.; Smallwood, R. J.; Welch, A. J. *J. Chem. Soc., Chem. Commun.* **1972**, 872.

(22) Panda, A.; Stender, M.; Olmstead, M. M.; Klavins, P.; Power, P. P. *Polyhedron* **2003**, *22*, 67.

(23) Putzer, M. A.; Neumüller, B.; Dehnicke, K.; Magull, J. *Ber. Bunsen-Ges.* **1996**, *129*, 715.

(24) Power, P. P. *Chem. Rev.* **2012**, *112*, 3482.

(25) Power, P. P. *Chemtracts* **1994**, *6*, 181.

(26) Lappert, M. F.; Power, P. P.; Sanger, A. R.; Srivastava, R. C. In *Metal and Metalloid Amides;* Horwood, E., Ed.; Chichester/Halsted Press: New York, 1980.

(27) Nguyen, T.; Panda, A.; Olmstead, M. M.; Richards, A. F.; Stender, M.; Brynda, M.; Power, P. P. *J. Am. Chem. Soc.* **2005**, *127*, 8545.

(28) Eichhöfer, A.; Hampe, O.; Lebedkin, S.; Weigend, F. *Inorg. Chem.* **2010**, *49*, 7331.

(29) Eichhöfer, A.; Buth, G.; Dolci, F.; Fink, K.; Mole, R. A.; Wood, P. T. *Dalton Trans.* **2011**, *40*, 7022.

(30) A paper which also contains investigations on the synthesis structure as well as electronic and dc magnetic properties of $[Co\{N(SiMe_3)_2\}_2(THF)]$ (**4**) and related trigonal-planar cobalt(II) complexes was published during the reviewing process of this Paper by Bryan, A. M.; Long, G. J.; Grandjean, F.; Power, P. P. *Inorg. Chem.* **2013**, *52*, 12152.

(31) Hursthouse, M. B.; Rodesiler, P. F. *J. Chem. Soc., Dalton Trans.* **1972**, 2100.

(32) Shannon, R. D. *Acta Crystallogr.* **1976**, *A32*, 751.

(33) Chilton, N. F.; Anderson, R. P.; Turner, L. D.; Soncini, A.; Murray, K. S. *J. Comput. Chem.* **2013**, *34*, 1164.

(34) McGarvey, B. R.; Telser, J. *Inorg. Chem.* **2012**, *51*, 6000.

(35) Gomez-Coca, S.; Cremades, E.; Aliaga-Alcalde, N.; Ruiz, E. *J. Am. Chem. Soc.* **2013**, *135*, 7010.

(36) Glauber, R. J. *J. Math. Phys.* **1963**, *4*, 294.

(37) Boča, R. *Coord. Chem. Rev.* **2004**, *248*, 757.

(38) Harriman, J. E. *Theoretical Foundations of Electron Spin Resonance;* Academic Press: New York, 1978.

(39) Boča, R.; Dlháň, L.; Linert, W.; Ehrenberg, H.; Fuess, H.; Haase, W. *Chem. Phys. Lett.* **1999**, *307*, 359.

(40) Jankovics, H.; Daskalakis, M.; Raptopoulou, C. P.; Terzis, A.; Tangoulis, V.; Giapintzakis, J.; Kiss, T.; Saligoglou, A. *Inorg. Chem.* **2002**, *41*, 3366.

(41) Atanasov, M.; Ganyushin, D.; Pantazis, D. A.; Sivalingam, K.; Neese, F. *Inorg. Chem.* **2011**, *50*, 7460.

(42) Palii, A. V.; Clemente-Juan, J. M.; Coronado, E.; Klokishner, S.; Ostrovsky, S.; Reu, O. S. *Inorg. Chem.* **2010**, *49*, 8073.

(43) Pointillart, F.; Bernot, K.; Sessoli, R.; Gatteschi, D. *Chem.—Eur. J.* **2007**, *13*, 1602.

(44) Ferbinteanu, M.; Kajiwara, T.; Choi, K.-Y.; Nojiri, H.; Nakamoto, A.; Kojima, N.; Cimpoesu, F.; Fujimura, Y.; Takaishi, S.; Yamashita, M. *J. Am. Chem. Soc.* **2006**, *128*, 9008.

(45) Gatteschi, D.; Sessoli, R.; Villain, J. *Molecular Nanomagnets;* Oxford University Press: Oxford, 2006.

(46) Koizumi, S.; Nihei, M.; Shiga, T.; Nakano, M.; Nojiri, H.; Bircher, R.; Waldmann, O.; Ochsenbein, S. T.; Güdel, H. U.; Fernandez-Alonso, F.; Oshio, H. *Chem.—Eur. J.* **2007**, *13*, 8445.

(47) Bendix, J.; Brorson, M.; Schäffer, C. E. *Inorg. Chem.* **1993**, *32*, 2838.

(48) Layfield, R. A.; McDouall, J. J. W.; Scheer, M.; Schwarzmaier, C.; Tuna, F. *Chem. Commun.* **2011**, *47*, 10623.

(49) Reiff, W. M.; Witten, E. H. *Polyhedron* **1984**, *3*, 443.

(50) Kramers, H. A. *Proc. R. Acad. Sci. Amsterdam* **1930**, *33*, 959.

(51) Cremades, E.; Ruiz, E. *Inorg. Chem.* **2011**, *50*, 4016.

(52) Companion, A. L.; Komorynskyl, M. A. *J. Chem. Educ.* **1964**, *41*, 257.
(53) Ribas Gispert, J. *Coordination Chemistry;* Wiley-VCH Verlag GmbH & Co. KGaA: Weinheim, 2008, p 265ff.
(54) Neese, F. *J. Chem. Phys.* **2007**, *127*, 164112.
(55) Neese, F. *Wiley Interdiscip. Rev.: Comput. Mol. Sci.* **2012**, *2*, 73.
(56) Maganas, D.; Sottini, S.; Kyritsis, P.; Groenen, E. J. J.; Neese, F. *Inorg. Chem.* **2011**, *50*, 8741.
(57) Neese, F. *J. Am. Chem. Soc.* **2006**, *128*, 10213−10222.
(58) Zein, S.; Duboc, C.; Lubitz, W.; Neese, F. *Inorg. Chem.* **2007**, *47*, 134.
(59) Alyea, E. C.; Bradley, D. C.; Copperthwaite, R. G.; Sales, K. D. *J. Chem. Soc., Dalton Trans.* **1973**, 185.
(60) Ellison, J.; Power, P. P.; Shoner, S. C. *J. Am. Chem. Soc.* **1989**, *111*, 8044.
(61) Lever, A. B. P. *Inorganic Electronic Spectroscopy*, 2nd ed., third impression; Elsevier: Amsterdam, 1984, p 448.
(62) MacDonnell, F. M.; Ruhland-Senge, K.; Ellison, J. J.; Holm, R. H.; Power, P. P. *Inorg. Chem.* **1995**, *34*, 1815.
(63) Evans, D. J.; Hughes, D. L.; Silver, J. *Inorg. Chem.* **1997**, *36*, 747.
(64) Day, B. M.; Pugh, T.; Hendriks, D.; Guerra, C. F.; Evans, D. J. F.; Bickelhaupt, M.; Layfield, R. A. *J. Am. Chem. Soc.* **2013**, *135*, 13338.
(65) *X-RED32 1.01, Data Reduction Program;* Stoe & Cie GmbH: Darmstadt, Germany, 2001.
(66) Sheldrick, G. M. *SHELXTL PC version 5.1 An Integrated System for Solving, Refining, and Displaying Crystal Structures from Diffraction Data;* Bruker Analytical X-ray Systems: Karlsruhe, 2000.
(67) *Diamond Version 2.1d, K.;* Crystal Impact GbR: Brandenburg, Germany, 1996−2000.
(68) *STOE, WinXPOW;* STOE & Cie GmbH: Darmstadt, Germany, 2000.
(69) Kahn, O. *Molecular Magnetism;* Wiley-VCH: Weinheim, Germany, 1993.
(70) Lueken, H. *Magnetochemie;* B. G. Teubner: Stuttgart, Leibzig, 1999 p 426.
(71) Haberditzl, W. *Angew. Chem.* **1966**, *78*, 277−288; *Angew. Chem., Int. Ed. Engl.* **1966**, *5*, 288−298.
(72) *TURBOMOLE V6.4;* TURBOMOLE GmbH: Karlsruhe, 2012, http://www.turbomole.de. TURBOMOLE is a development of University of Karlsruhe and Forschungszentrum Karlsruhe 1989−2007, TURBOMOLE GmbH since 2007.
(73) Treutler, O.; Ahlrichs, R. *J. Chem. Phys.* **1995**, *102*, 346.
(74) Eichkorn, K.; Treutler, O.; Oehm, H.; Häser, M.; Ahlrichs, R. *Chem. Phys. Lett.* **1995**, *240*, 283.
(75) Bauernschmitt, R.; Ahlrichs, R. *Chem. Phys. Lett.* **1996**, *256*, 454.
(76) Becke, A. D. *J. Chem. Phys.* **1993**, *98*, 5648.
(77) Perdew, J. P. *Phys. Rev. B* **1986**, *33*, 8822.
(78) Lee, C.; Yang, W.; Parr, R. G. *Phys. Rev. B* **1988**, *37*, 785.
(79) Weigend, F.; Ahlrichs, R. *Phys. Chem. Chem. Phys.* **2005**, *7*, 3297.
(80) Weigend, F. *Phys. Chem. Chem. Phys.* **2006**, *8*, 1057.